PHYSICAL REVIEW LETTERS

3D Sisyphus Cooling of Trapped Ions

S. Ejtemaee and P. C. Haljan[*]

Department of Physics, Simon Fraser University, Burnaby, British Columbia, V5A 1S6, Canada
(Received 1 March 2016; revised manuscript received 11 May 2017; published 25 July 2017)

Using a laser polarization gradient, we realize 3D Sisyphus cooling of $^{171}\text{Yb}^+$ ions confined in and near the Lamb-Dicke regime in a linear Paul trap. The cooling rate and final mean motional energy of a single ion are characterized as a function of laser intensity and compared to semiclassical and quantum simulations. Sisyphus cooling is also applied to a linear string of four ions to obtain a mean energy of 1–3 quanta for all vibrational modes, an approximately order of magnitude reduction below Doppler cooled energies. This is used to enable subsequent, efficient sideband laser cooling.

Applications of laser-cooled, trapped ions range from quantum information processing [1–6] and spectroscopy and metrology [7–10], to the study of interactions with cold atoms [11–16] and the study of few-body "phase transitions" [17–21]. Central to many of these applications is the manipulation of the collective vibrational modes of a string of Coulomb-coupled ions. The modes of interest are often required to be prepared in their quantum mechanical ground state, which is commonly achieved with sideband laser cooling [22–24] or electromagnetically induced transparency (EIT) cooling [25–27]. In practice, these techniques are implemented for reasons of efficiency in the Lamb-Dicke regime, where the ions' residual amplitude of vibration is small compared to the wavelength of the cooling laser [2,28,29]. Doppler laser precooling is usually sufficient to attain this condition, but if the trap is somewhat weaker, the ions will not begin close to the ground state, or deep in the Lamb-Dicke regime. For pulsed sideband cooling [23], this lengthens and complicates the sequence to walk the vibrational modes down the ladder of energy levels [30,31]. EIT cooling can provide a simplified cooling process, including a resonance width allowing simultaneous cooling of multiple modes [26,27], but its limited bandwidth poses a challenge for the cooling of modes widely spaced in frequency. Here we consider Sisyphus laser cooling, well known for neutral atoms [32], for the sub-Doppler cooling of trapped ions, in particular to act as a bridge between Doppler and ground-state laser cooling. This relaxes the requirement on trapping strength, which is of relevance for larger mass ions, and for the weaker axial confinement necessary for longer, linear ion strings, used, for example, in quantum simulations. Because of its nonresonant nature, Sisyphus cooling also offers a broadband technique for simultaneous, sub-Doppler cooling of trapped-ion vibrational modes. Furthermore, the specific implementation of Sisyphus cooling presented here for $^{171}\text{Yb}^+$ is of interest in explorations of cold atom-ion collisions in hybrid traps, where the heavier Yb^+ ion and a lighter atom is a favorable combination [33,34].

Since Sisyphus cooling was first demonstrated in a 3D optical molasses [35–38], the technique has been widely adopted to cool neutral atomic gasses to sub-Doppler temperatures [32]. Sisyphus cooling, primarily due to polarization gradients, has been used for the cooling and localization of atoms [39–50] in optical lattices [39–43], optical cavities [44,45], and optical tweezers [46–48], and as a more general technique it has been extended to the cooling of molecules in electric potentials [51], and the cooling of LC resonators coupled to a superconducting flux qubit [52]. Several early theoretical investigations, both semiclassical and quantum, extended the concept of Sisyphus cooling to a single ion confined in the Lamb-Dicke regime, with proposals considering cooling in both laser intensity [53,54] and polarization [55,56] gradients. Semiclassical simulations have also been used to study the final cooling energy in the crossover from the case of a bound ion in the Lamb-Dicke limit to the free-particle case [57]. Despite these theoretical works, the Sisyphus cooling of trapped ions has been reported only once, for one and two ions [58]. In this case, however, the confinement along the axis being cooled was so weak that the cooling was essentially the same as for free atoms.

In this Letter we realize the first 3D Sisyphus cooling of ions confined in and near the Lamb-Dicke regime. We characterize the cooling, based on a polarization gradient, as a function of laser intensity for a single ion. We then extend the technique to a linear string of four ions to demonstrate simultaneous cooling of all its vibrational modes. For our case of $^{171}\text{Yb}^+$ ions with an $F = 1 \rightarrow F = 0$ cooling transition [Fig. 1(a)], we construct a periodic polarization gradient in a transverse magnetic field as shown in Fig. 1(b) [59]. For high enough magnetic field (low enough intensity), the ground state coherences associated with coherent population trapping [60,61] can be ignored. A polarization gradient at the ion trap then gives rise to state-dependent light shift potentials and spatially dependent optical pumping such that a Sisyphus cooling effect occurs for blue detuning ($\Delta > 0$). A single-ion
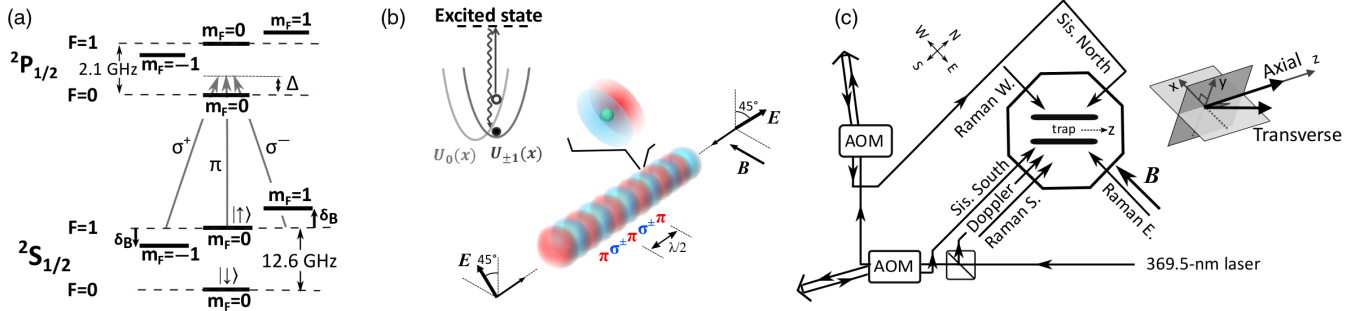
FIG. 1.   (a) Relevant energy levels of ^{171}Yb$^+$ for Sisyphus cooling. (b) An example of a single-ion Sisyphus cooling event from optical pumping between shifted harmonic trapping potentials associated with two effective sublevels of the $^2S_{1/2}|F=1\rangle$ ground state. The shift in potentials is due to dipole forces from the 1D polarization gradient shown, which is formed by counterpropagating, linearly polarized Sisyphus beams in a transverse magnetic field. (c) Laser beam configuration: Double-pass acousto-optic modulators (AOMs) are used to control the power and frequency of the Sisyphus beams, which enter the vacuum chamber and trap from the north and south sides. Perpendicular Raman beams entering from the east and south are used to probe ion motion in the axial ($\hat{z}$) trap direction; west and south beams are used for the transverse ($\hat{x}$ and $\hat{y}$) directions. Shown at right are the axial and transverse Raman wave vector directions overlaid on the principal axes of the trap.

cooling limit corresponding to a mean motional quantum number of $\bar{n} \approx 1$ is expected when the depth of the light shift potentials is on the order of the zero-point energy in the harmonic trap [55,57].

Our detailed studies of Sisyphus cooling with a single ^{171}Yb$^+$ ion are done in a linear Paul trap operating at a radio frequency of $\Omega_T/2\pi = 17.4$ MHz [61]. Typical secular trap frequencies are $\{\omega_x, \omega_y\}/2\pi = \{0.790, 0.766\}$ MHz in the transverse direction and $\omega_z/2\pi = 0.525$ MHz in the axial direction. An applied 5.9 G magnetic field gives a Zeeman shift of $\delta_B/2\pi = 8.2$ MHz between the $6s^2S_{1/2}|F=1, m_F\rangle$ sublevels. A laser beam detuned by -10 MHz of the $6s^2S_{1/2}(F=1) - 6p^2P_{1/2}(F=0)$ transition at $\lambda = 369.5$ nm provides fluorescence detection and Doppler cooling with $\bar{n} \sim 20$ in all trap directions. Optical pumping for initialization of the ion into the $^2S_{1/2}|0,0\rangle$ state is achieved with a laser modulation sideband driving the $^2S_{1/2}(F=1) - ^2P_{1/2}(F=1)$ transition.

A polarization-gradient field overlapping the trap is created by two counterpropagating and cross-polarized laser beams with $\sim$40-μm waists. The beams are derived from the Doppler cooling laser [Fig. 1(c)]. Acousto-optic modulators are used to obtain a detuning of $\Delta/2\pi = 310$ MHz above the $^2S_{1/2}(F=1) - ^2P_{1/2}(F=0)$ resonance and allow for independent adjustment of the power (< 45 μW) and frequency of the Sisyphus beams. The projections of either beam's wave vector along the trap directions ($v = \{x, y, z\}$) have magnitudes $k_v = (2\pi/\lambda)\{\frac{1}{2}, \frac{1}{2}, \frac{1}{\sqrt{2}}\}$ such that cooling is provided in three dimensions. The Lamb-Dicke parameters $\eta_v = k_v r_v$ in terms of the ground-state sizes $r_v = (\hbar/2m\omega_v)^{1/2}$ are $\{0.052, 0.053, 0.090\}$. The polarization of each beam is calibrated *in situ* from ac Stark shifts measured using microwave Ramsey interferometry between the $^2S_{1/2}|0,0\rangle \equiv |\downarrow\rangle$ and $^2S_{1/2}|1,0\rangle \equiv |\uparrow\rangle$ states. The single-beam intensities I, or, equivalently, on-resonant saturation

parameters $s_0 = I/(51$ mW/cm$^2)$, are also determined in this way, and are balanced to better than 10%. During Sisyphus cooling, the ion can be weakly optically pumped via the $^2P_{1/2}|F=1\rangle$ state into the dark $|\downarrow\rangle$ state and so out of the cooling cycle. To repump the ion, we use a pulsed sequence consisting of periods of Sisyphus cooling interleaved with reset operations composed of a 10-μs optical pumping pulse followed by a 90-μs microwave π pulse to prepare the ion in the $|\uparrow\rangle$ state. For optimal Sisyphus cooling of a single ion we should set the maximum of the polarization gradient at the center of the trap [53,55], which requires interferometric stability between the Sisyphus beams. Instead, we introduce a 0.080 MHz frequency difference between the beams to average over their relative phase—and its slow drifts—with a concomitant decrease in cooling rate and increase in cooling limit by approximately a factor of 2 [53,62].

The Sisyphus cooling is assessed with thermometry based on motion-sensitive, two-photon carrier transitions, for example, $|\downarrow\rangle|n_z\rangle \leftrightarrow |\uparrow\rangle|n_z\rangle$ [2]. A set of three off-resonant Raman beams (detuned by 100 GHz) allows us to obtain a carrier transition that is sensitive to motion in either the axial or transverse direction [see Fig. 1(c)]. The experiment sequence [Fig. 2(a)] involves 6.6 ms of Doppler cooling, then Sisyphus cooling, and finally thermometry operations. The thermometry involves the acquisition of a carrier Rabi oscillation with initialization via optical pumping to $|\downarrow\rangle$, and internal-state readout via state-sensitive fluorescence detection.

We first measure the Sisyphus cooling rate as a function of laser intensity. The cooling rate at each intensity value is extracted from a set of measurements of $\bar{n}$ at different Sisyphus cooling times, where the value of $\bar{n}$ at each time is obtained from a fit to the carrier Rabi oscillation [Figs. 2(b)–2(e)]. We vary the Sisyphus cooling time by varying the number of Sisyphus pulses with their duration
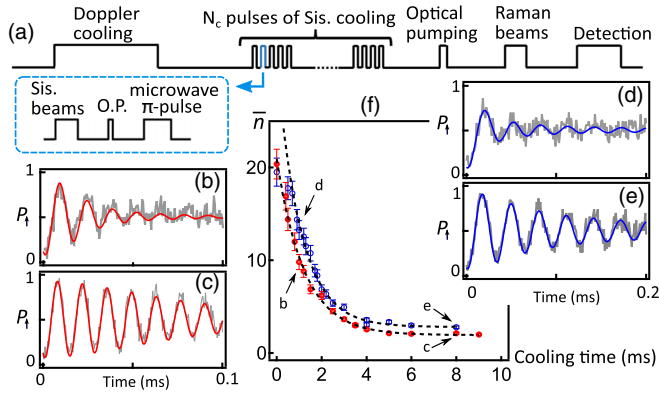
FIG. 2. (a) Experiment sequence for assessing Sisyphus cooling of a single trapped ion. Each step of the N_c-pulse Sisyphus sequence involves a cooling pulse and a reset (i.e., repump) to the $|\uparrow\rangle$ state using optical pumping (OP) and microwave pulses. (b)–(e) Raman carrier Rabi oscillations in the (b)–(c) transverse and (d)–(e) axial directions with cooling times of [(b),(d)] 10×0.1 and [(c),(e)] 80×0.1 ms. Gray lines are the measured probability $P_\uparrow$ of obtaining $|\uparrow\rangle$ averaged over 50 runs per time value. Red and blue lines are fits to extract $\bar{n}$. (f) Cooling dynamics for transverse (red) and axial (blue) directions at $s_0 = 11$. Error bars are statistical uncertainties from fits. Dashed lines are exponential fits used to extract the cooling rate. Only points with $\bar{n} \leq 15$ are considered to omit the initial cooling dynamics.

kept constant. The pulse duration for a given beam intensity is set to keep the probability of pumping out of the cooling cycle to 15%. The fit function for the Rabi oscillation assumes an initial thermal distribution of motional Fock states and includes fixed corrections for detection efficiencies. The only free fit parameters are $\bar{n}$ and a carrier Rabi frequency scale. In the transverse direction, our Raman setup couples to both x and y motions with equal Raman wave vector projection onto each axis [Fig. 1(c)]. We use an approximate 2D model for the transverse fits in which we assume the same $\bar{n}$ for both axes and ignore the effect of Raman transitions related to cross-mode coupling between the axes [2]. Even though we do not resolve the closest of these transitions to the carrier, simulations show that the fit model is adequate for the $\bar{n}$ range considered ($\leq 5\%$ systematic effect at highest $\bar{n}$ values) [62].

Typical cooling dynamics at $s_0 = 11$ are shown in Fig. 2(f) for both the axial and transverse directions. An exponential fit is used to extract a cooling time constant τ. Since on average the ion is cooled 85% of the time, due to the effect of pumping dark, our plotted cooling rate is calculated as $\Gamma_c = (\tau/0.85)^{-1}$. Figures 3(a)–3(b) show the intensity dependence of the axial and transverse cooling rates. The cooling rates in the two directions compare within a factor of 2 of each other over the measured range, spanning more than a factor of 40. Power-law fits of the axial and transverse data give exponents 1.98(6) and 1.91(3) respectively, which match well with the expected s_0^2 scaling in the Lamb-Dicke regime and in the absence of coherences between Zeeman levels [55,62].
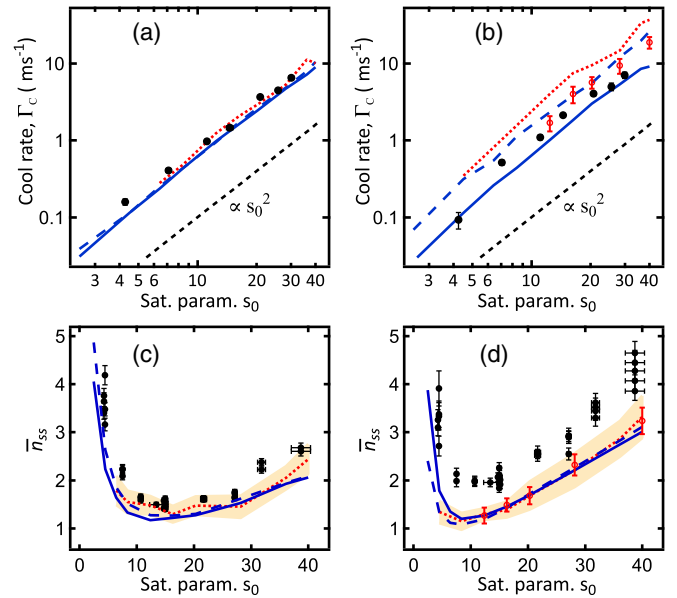

FIG. 3. Sisyphus cooling rate Γ_c (top) and steady-state mean phonon number $\bar{n}_{ss}$ (bottom) as a function of a single-beam saturation parameter s_0 for the transverse direction (left) and axial direction (right). Panels include experimental data (black filled circles) and predictions from 1D (dashed blue line) and 3D (solid blue line) semiclassical simulations, and 1D quantum simulations with initial $n_i = 8$ Fock state (dotted red line) and initial $\bar{n} = 22$ thermal state (red circles). Semiclassical simulations average over 1000 Monte Carlo runs. Quantum simulations average over 40 (80) runs for Fock (thermal) initial states. Vertical error bars for data are statistical uncertainties from fits, and horizontal error bars account for calibration uncertainty and drifts in laser intensity. In (b), error bars for the quantum simulation with the thermal initial state are bootstrap uncertainties. Shaded error bands and error bars for quantum simulations in (c) and (d) show the standard deviation of fluctuations at the steady state.

Next, we measure the steady-state mean occupation number $\bar{n}_{ss}$ as a function of laser intensity. Potential heating sources such as micromotion and laser power noise are minimized on a regular basis. At each intensity, the single-pulse cooling time is set to keep the probability of pumping out of the cooling cycle at a fixed value of 20%, and a cooling time in excess of 9τ is chosen to allow the energy of the ion to reach equilibrium. Figures 3(c)–3(d) show the intensity dependence of $\bar{n}_{ss}$ for both the axial and transverse directions. In each case, a cooling limit of $\bar{n}_{ss} \simeq 1.5$–2 is obtained at an optimum intensity. The lower optimum intensity in the less strongly confined axial direction is consistent with the theoretical expectation for an ion in the Lamb-Dicke regime [53,55].

Both semiclassical and quantum simulations are performed to assess the experimental results. For all simulations the trap is treated in the pseudopotential approximation, and a 0.080 MHz frequency difference between the Sisyphus beams is included. We consider both 1D and 3D semiclassical Monte Carlo simulations, which treat the motion of the ion classically and include a period

of Doppler cooling followed by Sisyphus cooling to match the experiment. The Sisyphus cooling model follows the rate-equation approach of Ref. [57] with the appropriate diffusion heating terms calculated according to Refs. [63,64]. The effect of photon scattering from the $^2P_{1/2}|F = 1\rangle$ states, which is omitted in the simulations, is included in the $\bar{n}_{ss}$ values presented through an intensity-dependent correction determined analytically [62]. The quantum simulation is implemented in one dimension with the Monte Carlo wave function method [65] according to Ref. [66]. It includes the hyperfine structure of the $^2S_{1/2}$–$^2P_{1/2}$ transition and coherences between Zeeman levels, but ignores any coherences between F levels. The $^2S_{1/2}|0, 0\rangle$ state is effectively eliminated by assuming an instantaneous recoilless repump. The majority of our quantum simulations use an initial Fock state of $n_i = 8$ and are limited to a Hilbert space of 20 motional n levels in order to restrict the computational time required. A limited subset of points is repeated with a thermal initial state at Doppler temperature and a Hilbert space of 200 n levels.

For the transverse cooling rate [Fig. 3(a)], all the simulation models match the experimental results fairly well. In the weaker axial direction [Fig. 3(b)], the 3D semiclassical simulation matches the data better overall than the 1D semiclassical simulation and distinctly better than the quantum simulation with $n_i = 8$. The discrepancy between the 1D and 3D semiclassical simulations (by a factor of 2–3) suggests that the axial cooling behavior is affected by the transverse motion, perhaps due to motional coupling or due to the additional delocalization of the ion. Simulations in a tighter trap by a factor of 3 (that is deeper in the Lamb-Dicke regime) do not show this difference. The higher axial cooling rate predicted by the 1D quantum simulation with $n_i = 8$, by an overall factor of 3–4, is related to the lower initial motional energy used in the calculation. As shown in Fig. 3(b), a thermal initial state with a Doppler cooled value of $\bar{n} = 22$ brings the quantum result in line with the 1D semiclassical simulation and closer to the experimental data, indicating the effect of deviations from the Lamb-Dicke regime in the early cooling dynamics.

For the transverse $\bar{n}_{ss}$ in Fig. 3(c), the quantum and semiclassical simulations lie close to one another and only show a small discrepancy with the data over the intensity range considered. In the axial direction, there is a much stronger discrepancy between the experiment and theory by up to a factor of 2, although the general behaviors still agree. While the source of the discrepancies remains to be identified, we have verified that the carrier thermometry does not present a measurement limit.

In the final experiment, we extend Sisyphus cooling to a linear string of ions, specifically $N = 4$ ions confined in a slightly weaker axial trap with $\omega_z/2\pi = 0.34$ MHz. All the ions in the 16-μm long string interact with the polarizaton gradient field. We choose $s_0 = 15$ and apply the cooling for a duration of 30×0.2 ms. The experimental sequence is the same as for a single ion; however, for thermometry of
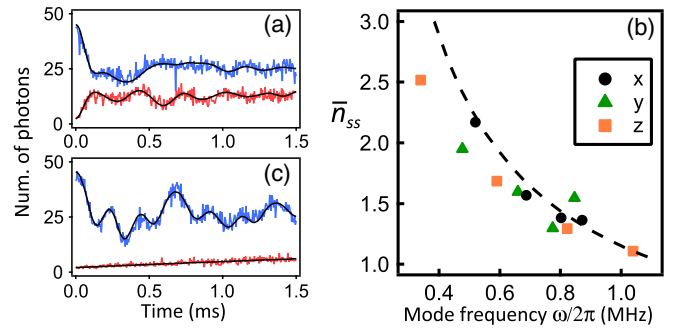

FIG. 4.   (a) Raman Rabi oscillations on the first red sideband transition for the y-zigzag vibrational mode ($\omega/2\pi = 0.48$ MHz) in a Sisyphus-cooled linear string of four ^{171}Yb$^+$ ions. The initial internal state is either $|\downarrow, \downarrow, \downarrow, \downarrow\rangle$ (red) or $|\uparrow, \uparrow, \uparrow, \uparrow\rangle$ (blue). Vertical scale proportional to the number of ions in $|\uparrow\rangle$ averaged over 50 runs. Black lines are a combined fit to extract $\bar{n}_{ss} = 2.0$ and include approximate models for optical pumping and contrast loss for red and blue curves, respectively. (b) Mean phonon number for all four-ion vibrational modes following Sisyphus cooling at $s_0 = 15$. Trap frequencies $\{0.84, 0.87, 0.34\}$ MHz. Dashed line shows ω^{-1} scaling for reference. (c) Same mode as (a) but Sisyphus then sideband cooled ($\bar{n} \leq 0.05$ from fit).

each vibrational normal mode, we measure red-sideband Raman oscillations starting from either the $|\downarrow\downarrow\downarrow\downarrow\rangle$ or the $|\uparrow\uparrow\uparrow\uparrow\rangle$ state, and fit the oscillations together to find $\bar{n}_{ss}$ for an assumed thermal distribution [67]. The Raman beams nominally uniformly illuminate the ions. Figure 4(a) shows an example of the Rabi oscillations for the y-axis zigzag mode. The fit function ignores spectator-mode effects [2], which are expected to be small given that all modes are Sisyphus cooled. We also modify the fit function to account for experimental imperfections in the Raman transition, including optical pumping as a result of spontaneous emission and loss of contrast due to residual intensity inhomogeneities across the ion string. Figure 4(b) shows the mean vibrational number $\bar{n}_{ss}$ following Sisyphus cooling for all of the $3N$ normal modes as a function of their frequency. The Sisyphus cooling reduces the energy of all modes to $\bar{n}_{ss} \leq 3$. Starting from the Sisyphus cooled string, we have implemented separate sideband cooling of all modes with a typical result of $\bar{n} \leq 0.05$ [for example, Fig. 4(c)].

In summary, Sisyphus laser cooling has been used to reduce the thermal energy of trapped ions in three dimensions by approximately an order of magnitude, thereby bridging Doppler and sideband cooling in our setup. In addition to providing near ground-state cooling, Sisyphus cooling benefits from a simplicity and robustness because it is not a resonant process, and so does not require fine-tuning of multiple cooling parameters. The Sisyphus technique is convenient to implement since it requires only modest optical power and uses the same single direction of optical access as for Doppler cooling, and it is technically easier to implement for ^{171}Yb$^+$ than EIT cooling due to the ion's energy-level structure. Compared to EIT cooling, which can provide

simultaneous ground-state cooling of multiple vibrational modes clustered in frequency [26,27], Sisyphus cooling is broader band since it is a nonresonant technique. It does not, however, achieve as high cooling rates or as low final energies as an EIT cooling setup that is optimized for narrow band operation [68]. For longer ion strings, the efficiency of EIT cooling for low-frequency modes starting far outside the Lamb-Dicke regime is unclear [27]. Further investigation of the Sisyphus cooling performance with respect to a range of parameters, and the crossover to behavior outside the Lamb-Dicke regime [57], will be presented elsewhere [62]. The Sisyphus technique should immediately extend to ion strings at least moderately larger than four ions. This opens up the possibility in our setup to explore dynamics of the linear-zigzag transition in and near the quantum regime [69], and should be of interest for recent proposals to study heat transport in ion strings [70–74]. Sisyphus cooling may also be useful in quantum information applications where ground-state cooling is not required, for example, in microwave-based quantum logic [75–77] or other proposed schemes [78,79].

---

*Corresponding author.
phaljan@sfu.ca

[1] J. I. Cirac and P. Zoller, Phys. Rev. Lett. **74**, 4091 (1995).

[2] D. Wineland, C. Monroe, W. M. Itano, D. Leibfried, B. E. King, and D. M. Meekhof, J. Res. Natl. Inst. Stand. Technol. **103**, 259 (1998).

[3] R. Blatt and D. Wineland, Nature (London) **453**, 1008 (2008).

[4] M. Johanning, A. Braun, N. Timoney, V. Elman, W. Neuhauser, and C. Wunderlich, Phys. Rev. Lett. **102**, 073004 (2009).

[5] R. Islam, E. Edwards, K. Kim, S. Korenblit, C. Noh, H. Carmichael, G.-D. Lin, L.-M. Duan, C.-C. Joseph Wang, J. Freericks, and C. Monroe, Nat. Commun. **2**, 377 (2011).

[6] R. Blatt and C. F. Roos, Nat. Phys. **8**, 277 (2012).

[7] T. Schneider, E. Peik, and C. Tamm, Phys. Rev. Lett. **94**, 230801 (2005).

[8] C. F. Roos, M. Chwalla, K. Kim, M. Riebe, and R. Blatt, Nature (London) **443**, 316 (2006).

[9] T. Rosenband, D. B. Hume, P. O. Schmidt, C. W. Chou, A. Brusch, L. Lorini, W. H. Oskay, R. E. Drullinger, T. M. Fortier, J. E. Stalnaker, S. A. Diddams, W. C. Swann, N. R. Newbury, W. M. Itano, D. J. Wineland, and J. C. Bergquist, Science **319**, 1808 (2008).

[10] K. Hosaka, S. A. Webster, A. Stannard, B. R. Walton, H. S. Margolis, and P. Gill, Phys. Rev. A **79**, 033403 (2009).

[11] W. W. Smith, O. P. Makarov, and J. Lin, J. Mod. Opt. **52**, 2253 (2005).

[12] A. T. Grier, M. Cetina, F. Oručević, and V. Vuletić, Phys. Rev. Lett. **102**, 223201 (2009).

[13] S. Schmid, A. Härter, and J. H. Denschlag, Phys. Rev. Lett. **105**, 133202 (2010).

[14] C. Zipkes, S. Palzer, C. Sias, and M. Kohl, Nature (London) **464**, 388 (2010).

[15] S. Haze, R. Saito, M. Fujinaga, and T. Mukaiyama, Phys. Rev. A **91**, 032709 (2015).

[16] A. Hrter and J. H. Denschlag, Contemp. Phys. **55**, 33 (2014).

[17] S. Ejtemaee and P. C. Haljan, Phys. Rev. A **87**, 051401 (2013).

[18] K. Pyka, J. Keller, H. L. Partner, R. Nigmatullin, T. Burgermeister, D. M. Meier, K. Kuhlmann, A. Retzker, M. B. Plenio, W. H. Zurek, A. del Campo, and T. E. Mehlstäubler, Nat. Commun. **4** (2013).

[19] S. Ulm, J. Roßnagel, G. Jacob, C. Degnther, S. T. Dawkins, U. G. Poschinger, R. Nigmatullin, A. Retzker, M. B. Plenio, F. Schmidt-Kaler, and K. Singer, Nat. Commun. **4**, 2290 (2013).

[20] M. B. Plenio and A. Retzker, Ann. Phys. (Amsterdam) **525**, A159 (2013).

[21] A. Bylinskii, D. Gangloff, and V. Vuletic, Science **348**, 1115 (2015).

[22] F. Diedrich, J. C. Bergquist, W. M. Itano, and D. J. Wineland, Phys. Rev. Lett. **62**, 403 (1989).

[23] C. Monroe, D. M. Meekhof, B. E. King, S. R. Jefferts, W. M. Itano, D. J. Wineland, and P. Gould, Phys. Rev. Lett. **75**, 4011 (1995).

[24] B. E. King, C. S. Wood, C. J. Myatt, Q. A. Turchette, D. Leibfried, W. M. Itano, C. Monroe, and D. J. Wineland, Phys. Rev. Lett. **81**, 1525 (1998).

[25] C. F. Roos, D. Leibfried, A. Mundt, F. Schmidt-Kaler, J. Eschner, and R. Blatt, Phys. Rev. Lett. **85**, 5547 (2000).

[26] Y. Lin, J. P. Gaebler, T. R. Tan, R. Bowler, J. D. Jost, D. Leibfried, and D. J. Wineland, Phys. Rev. Lett. **110**, 153002 (2013).

[27] R. Lechner, C. Maier, C. Hempel, P. Jurcevic, B. P. Lanyon, T. Monz, M. Brownnutt, R. Blatt, and C. F. Roos, Phys. Rev. A **93**, 053401 (2016).

[28] D. Leibfried, R. Blatt, C. Monroe, and D. Wineland, Rev. Mod. Phys. **75**, 281 (2003).

[29] J. Eschner, G. Morigi, F. Schmidt-Kaler, and R. Blatt, J. Opt. Soc. Am. B **20**, 1003 (2003).

[30] G. Poulsen, Y. Miroshnychenko, and M. Drewsen, Phys. Rev. A **86**, 051402 (2012).

[31] Y. Wan, F. Gebert, F. Wolf, and P. O. Schmidt, Phys. Rev. A **91**, 043425 (2015).

[32] H. J. Metcalf and P. van der Straten, *Laser Cooling and Trapping* (Springer, New York, 1999).

[33] M. Cetina, A. T. Grier, and V. Vuletić, Phys. Rev. Lett. **109**, 253201 (2012).

[34] T. V. Tscherbul, P. Brumer, and A. A. Buchachenko, Phys. Rev. Lett. **117**, 143201 (2016).

[35] P. D. Lett, R. N. Watts, C. I. Westbrook, W. D. Phillips, P. L. Gould, and H. J. Metcalf, Phys. Rev. Lett. **61**, 169 (1988).

[36] J. Dalibard and C. Cohen-Tannoudji, J. Opt. Soc. Am. B **6**, 2023 (1989).

[37] P. J. Ungar, D. S. Weiss, E. Riis, and S. Chu, J. Opt. Soc. Am. B **6**, 2058 (1989).

[38] In general the Sisyphus effect is not the only polarization-gradient cooling mechanism in optical molasses; see Ref. [36].

[39] P. S. Jessen, C. Gerz, P. D. Lett, W. D. Phillips, S. L. Rolston, R. J. C. Spreeuw, and C. I. Westbrook, Phys. Rev. Lett. **69**, 49 (1992).

[40] P. Verkerk, B. Lounis, C. Salomon, C. Cohen-Tannoudji, J.-Y. Courtois, and G. Grynberg, Phys. Rev. Lett. **68**, 3861 (1992).

[41] A. Kastberg, W. D. Phillips, S. L. Rolston, R. J. C. Spreeuw, and P. S. Jessen, Phys. Rev. Lett. **74**, 1542 (1995).

[42] S. L. Winoto, M. T. DePue, N. E. Bramall, and D. S. Weiss, Phys. Rev. A **59**, R19 (1999).

[43] W. S. Bakr, A. Peng, M. E. Tai, R. Ma, J. Simon, J. I. Gillen, S. Flling, L. Pollet, and M. Greiner, Science **329**, 547 (2010).

[44] S. Nuszmann, K. Murr, M. Hijlkema, B. Weber, A. Kuhn, and G. Rempe, Nat. Phys. **1**, 122 (2005).

[45] A. D. Boozer, A. Boca, R. Miller, T. E. Northup, and H. J. Kimble, Phys. Rev. Lett. **97**, 083602 (2006).

[46] N. Schlosser, G. Reymond, I. Protsenko, and P. Grangier, Nature (London) **411**, 1024 (2001).

[47] M. McGovern, A. J. Hilliard, T. Grünzweig, and M. F. Andersen, Opt. Lett. **36**, 1041 (2011).

[48] A. M. Kaufman, B. J. Lester, and C. A. Regal, Phys. Rev. X **2**, 041014 (2012).

[49] B. Sheehy, S.-Q. Shang, P. van der Straten, S. Hatamian, and H. Metcalf, Phys. Rev. Lett. **64**, 858 (1990).

[50] Y. B. Ovchinnikov, I. Manek, and R. Grimm, Phys. Rev. Lett. **79**, 2225 (1997).

[51] M. Zeppenfeld, B. G. U. Englert, R. Glockner, A. Prehn, M. Mielenz, C. Sommer, L. D. van Buuren, M. Motsch, and G. Rempe, Nature (London) **491**, 570 (2012).

[52] M. Grajcar, S. H. W. van der Ploeg, A. Izmalkov, E. Il'ichev, H.-G. Meyer, A. Fedorov, A. Shnirman, and G. Schon, Nat. Phys. **4**, 612 (2008).

[53] D. J. Wineland, J. Dalibard, and C. Cohen-Tannoudji, J. Opt. Soc. Am. B **9**, 32 (1992).

[54] J. I. Cirac, R. Blatt, P. Zoller, and W. D. Phillips, Phys. Rev. A **46**, 2668 (1992).

[55] J. I. Cirac, R. Blatt, A. S. Parkins, and P. Zoller, Phys. Rev. A **48**, 1434 (1993).

[56] S. M. Yoo and J. Javanainen, Phys. Rev. A **48**, R30 (1993).

[57] Y. Li and Mølmer, Laser Phys. **4**, 829 (1994).

[58] G. Birkl, J. A. Yeazell, R. Rückerl, and H. Walther, Europhys. Lett. **27**, 197 (1994).

[59] P. van der Straten, S.-Q. Shang, B. Sheehy, H. Metcalf, and G. Nienhuis, Phys. Rev. A **47**, 4160 (1993).

[60] D. J. Berkeland and M. G. Boshier, Phys. Rev. A **65**, 033413 (2002).

[61] S. Ejtemaee, R. Thomas, and P. C. Haljan, Phys. Rev. A **82**, 063419 (2010).

[62] S. Ejtemaee and P. C. Haljan (to be published).

[63] J. P. Gordon and A. Ashkin, Phys. Rev. A **21**, 1606 (1980).

[64] G. Nienhuis, P. van der Straten, and S.-Q. Shang, Phys. Rev. A **44**, 462 (1991).

[65] J. Dalibard, Y. Castin, and K. Mølmer, Phys. Rev. Lett. **68**, 580 (1992).

[66] J. Johansson, P. Nation, and F. Nori, Comput. Phys. Commun. **184**, 1234 (2013).

[67] This is equivalent to thermometry based on the red and blue sidebands described in Ref. [28].

[68] For EIT cooling, bandwidth can be increased, but at the expense of cooling rate and limit. see Ref. [27].

[69] A. Retzker, R. C. Thompson, D. M. Segal, and M. B. Plenio, Phys. Rev. Lett. **101**, 260504 (2008).

[70] G.-D. Lin and L.-M. Duan, New J. Phys. **13**, 075015 (2011).

[71] T. Pruttivarasin, M. Ramm, I. Talukdar, A. Kreuter, and H. Hffner, New J. Phys. **13**, 075012 (2011).

[72] A. Bermudez, M. Bruderer, and M. B. Plenio, Phys. Rev. Lett. **111**, 040601 (2013).

[73] N. Freitas, E. Martinez, and J. P. Paz, Phys. Scr. **91**, 013007 (2015).

[74] A. Ruiz, D. Alonso, M. B. Plenio, and A. del Campo, Phys. Rev. B **89**, 214305 (2014).

[75] C. Ospelkaus, U. Warring, Y. Colombe, K. R. Brown, J. M. Amini, D. Leibfried, and D. J. Wineland, Nature (London) **476**, 181 (2011).

[76] N. Timoney, I. Baumgart, M. Johanning, A. F. Varon, M. B. Plenio, A. Retzker, and C. Wunderlich, Nature (London) **476**, 185 (2011).

[77] S. C. Webster, S. Weidt, K. Lake, J. J. McLoughlin, and W. K. Hensinger, Phys. Rev. Lett. **111**, 140501 (2013).

[78] G.-D. Lin, S.-L. Zhu, R. Islam, K. Kim, M.-S. Chang, S. Korenblit, C. Monroe, and L.-M. Duan, Europhys. Lett. **86**, 60004 (2009).

[79] J. D. Baltrusch, C. Cormick, G. De Chiara, T. Calarco, and G. Morigi, Phys. Rev. A **84**, 063821 (2011).